

# Dynamic Human Gait Phase Detection Algorithm

Luan V. Nguyen, Hung M. La and Trung H. Duong

**Abstract**—Human foot motion localization based on Inertial Measurement Unit (IMU) sensor especially in large environments has many potential applications such as search and rescue in fire or in emergency, navigation for visitor and security purposes, etc. However, current existing algorithms are so far from practical applications. Because they usually apply a fixed threshold for human gait phase detection, they can not work with different speeds of human motion in real-time practical applications. In this paper, we propose a Dynamic Gait Phase (DGP) detection algorithm for different speeds of human foot motion. Our DGP detection algorithm can recognize accurate detection of the stance and swing phases of human gait in different foot motion speeds. This advantage supports to estimate accurately the human foot position in a real-time manner. The DGP detection algorithm has been validated by the Motion Tracking System (Ground Truth). Experimental results have been conducted to detect the stance and swing phases of the human gait with dynamic speeds of human foot motion.

**Keywords:** Gait phase detection, Human foot motion localization, Zero velocity update, Inertial navigation system.

## I. INTRODUCTION

The tracking of human foot motion trajectory can be implemented by different methods and technologies (e.g. ultrasound, wireless, radio and vision technology, etc). One popular method for human foot localizations in indoor environments is a Pedestrian Dead-Reckoning (PDR) [1]. The localization systems relied on PDR are simple and do not need to setup any infrastructure. They have just relied on the knowledge of walking gait phase detection of PDR and a light and wearable inertial sensor such as an IMU mounted on a foot. Since the Micro Electro Mechanical System (MEMS) technology has been born, the human foot motion tracking based on the Inertial/Magnetic Measurement Units (IMMUs) sensors has been researched and has some significantly published results [2]–[5]. This method is implemented simply and conveniently by mounting a small IMU sensor on shoe. It integrates the position of foot motion from IMU data by a Inertial Navigation System (INS). This technique usually applies a Gait Phase Detection and Zero Velocity Update (ZVU) together for its integrated process. Obviously, the accuracy of INS process depends very much on its ability to detect correctly the gait phase of human foot motion.

There are many applications of localization and navigation of human foot motion [6]–[9]. However, reaching high accuracy of human foot motion localization based on the IMU sensors especially in the environments with local magnetic disturbances is a challenging research topic. There are some existing work [3]–[5] researched on and proposed the solutions to increase the

accuracy of human foot motion localization based on the IMU sensors. The accuracy of human foot motion trajectory using IMU is variety, and its error is usually greater than 10% of total travel length. Besides, the localization algorithms for mobile devices and wearable sensor on human motion were proposed [10], [11]. In summary, the existing algorithms have some disadvantages as they are usually off-line algorithms which are designed to work only on off-line data set. Additionally, they only detect the gait of human motion for a normal or certain foot motion speed. Hence, they can not work with different speeds of human motion in real-time practical applications. In this paper, we focus on the development of a Dynamic Gait Phase (DGP) detection algorithm for human foot motion localization. The proposed algorithm can work with different motion speeds so that the human foot motion localization can achieve higher accuracy in real-time applications.

The main contribution of this paper is the development of DGP detection algorithm for different speeds of real-time human foot motion. We propose an efficient method to detect gait phases of human foot motion in which the threshold values are automatically computed and updated by real-time human motion speeds. These dynamic threshold updates can help the DGP detection algorithm work with any human motion speed like walking or running.

The remaining of the paper is organized as follows. The next section presents dynamic gait phase detection algorithm. Section III presents experiments and use of the Motion Tracking System to verify accuracy of the proposed DGP detection algorithm. Finally, the conclusion is given in Section IV.

## II. DYNAMIC GAIT PHASE DETECTION (DGP)

Due to the drift of real-time IMU data of acceleration, angular rate and magnetic field, we can not solely rely on the INS to estimate the position of human foot. Besides, the IMU drift is also effected by the position, attitude on the Earth and the objects in surrounding environments such as steel frame inside building and moving objects, etc. Luckily, this drift can be detected and reduced by ZVU algorithm. This algorithm rely on the accuracy of human motion gait phases detection. Otherwise, it is worth to note that human gait is composed by two phases, stance and swing phases [12] as show in Fig. 1. In the stance phase, human foot stands on the ground and it doesn't move. This means that the actual velocity of human foot in this phase must be zero. Hence, if the velocity of the foot is detected larger than zero in this phase, it must be the error velocity coming from IMU drift.

The human gait phase definitely depends on the different people and motion speed. Higher speeds are shorter gait phases. There is a very important question of how to detect the stance phase of each human gait in different motion speeds. In [4] the stance phase detection algorithm is limited to normal walking

L. Nguyen and H. La are with the Department of Computer Science and Engineering, University of Nevada, Reno, NV 89557, USA. Corresponding author: Hung La, email: hla@unr.edu.

T. Duong is with the Center for Advanced Infrastructure and Transportation, Rutgers University, Piscataway, NJ 08854, USA.

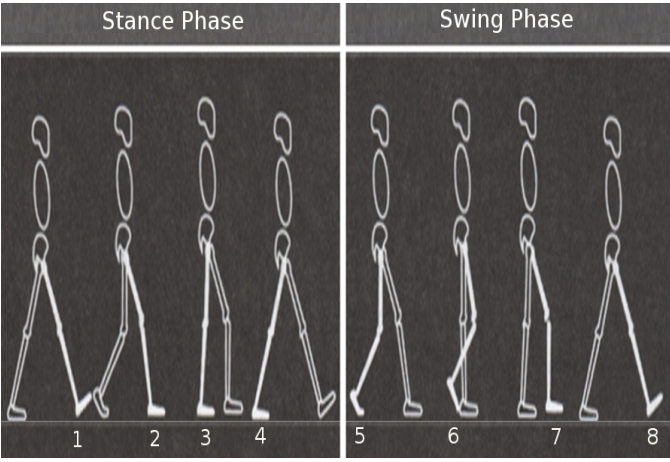


Fig. 1. Human Motion Gait Phases

speed motion. It may not work for fast or slow changing speeds than normal speed. In [3] a method using both acceleration and angular rate to check for stance phase of human gait is proposed. This method requires some pre-determined thresholds for checking the magnitude of acceleration, local acceleration, and gyroscope. Obviously, it will meet problem with different people and different speeds of motion. In this paper, we propose an efficient method to detect gait phases of human foot motion in which the threshold values are automatically computed and updated by real-time human motion speeds. Therefore, our proposed algorithm can work with any human motion speed like walking or running.

We firstly presents the dynamics of sensor data. They include the change of local acceleration ( $|\mathbf{a}_{local,i}^{t+1} - \mathbf{a}_{local,i}^t|$ ), of magnitude of acceleration ( $|\mathbf{a}_{m,i}^{t+1} - \mathbf{a}_{m,i}^t|$ ), and of angular rate magnitude ( $|\mathbf{w}_{m,i}^{t+1} - \mathbf{w}_{m,i}^t|$ ) at time  $t + 1$  of step  $i$ .

Then the dynamic  $d_{g,i}^{t+1}$  at time  $t + 1$  of step  $i$  can be defined:

$$d_{g,i}^{t+1} = |\mathbf{a}_{local,i}^{t+1} - \mathbf{a}_{local,i}^t| + |\mathbf{a}_{m,i}^{t+1} - \mathbf{a}_{m,i}^t| + |\mathbf{w}_{m,i}^{t+1} - \mathbf{w}_{m,i}^t|. \quad (1)$$

where, the local acceleration  $\mathbf{a}_{local,i}^{t+1}$  is computed:

$$(\mathbf{a}_{local,i}^{t+1})^2 = \frac{1}{2s+1} \sum_{j=t-2s}^{t+1} (\mathbf{a}_{b,i}^{t+1} - \mathbf{a}_{ave,i}^j)^2. \quad (2)$$

where, the  $\mathbf{a}_{b,i}^{t+1}$  is an acceleration of IMU in its body frame at time  $t + 1$  of step  $i$ . Note that Equ. (2) is computed in real-time and we just need data for computing local acceleration from some previous time steps. This is a main difference comparing to the off-line algorithms in [4] [3], [5]. Superindex  $j$  in Equ. (2) above is from time  $t + 1$  dating back to  $(2s + 1)$  previous time steps.

The average acceleration  $\mathbf{a}_{ave,i}^j$  in Equ. (2) is computed by:

$$\mathbf{a}_{ave,i}^j = \frac{1}{2s+1} \sum_{k=j-2s-1}^j \mathbf{a}_{b,i}^k. \quad (3)$$

Then the dynamic gain  $d_{g,i}^{t+1}$  at times  $t + 1$  of steps  $i$  is used to compute the values of stance condition  $s_{c,i}^{t+1}$  from the five nearest previous values of  $d_{g,i}^{t+1}$ :

$$s_{c,i}^{t+1} = \frac{d_{g,i}^{t+1} + d_{g,i}^t + d_{g,i}^{t-1} + d_{g,i}^{t-2} + d_{g,i}^{t-3}}{5}. \quad (4)$$

We define  $\mathbf{s}_{c,(i-1)}$  as an array of all discretized points  $s_{c,(i-1)}^{t+1}$  during the swing phase of step  $(i - 1)$ . Please see the green line in the Swing Phase of Fig. 2.

We assume that  $t + 1$  is a discretized time during step  $i$  of motion. The delay of stance condition  $s_{d,i}^{t+1}$  of  $s_{c,i}^{t+1}$  is obtained:

$$s_{d,i}^{t+1} = \frac{s_{d,i}^{t-1} + s_{c,i}^{t+1}}{2}, \quad (5)$$

where, the initial value of  $s_{d,i}^0$  can be initiated by 0.8. We define  $\mathbf{s}_{d,(i-1)}$  as an array of all discretized points  $s_{d,(i-1)}^{t+1}$  during the swing phase of step  $(i - 1)$ . Please see the red line in the Swing Phase of Fig. 2.

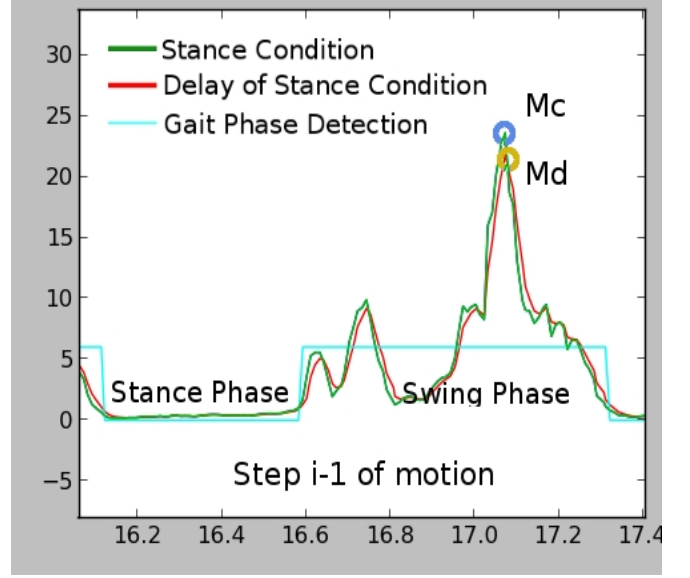


Fig. 2. Human gait phases detection at step  $i-1$

We name  $max_{cd,i}^{t+1}$  as the Max Changing Speed for the difference between  $s_{d,i}^{t+1}$  and  $s_{c,i}^{t+1}$ . It can be obtained by formula:

$$max_{cd,i}^{t+1} = \begin{cases} s_{c,i}^{t+1}, & s_{d,i}^{t+1} \leq s_{c,i}^{t+1} \\ s_{d,i}^{t+1}, & otherwise. \end{cases} \quad (6)$$

We define  $Mc(\mathbf{s}_{c,(i-1)})$  as a maximum value of the stance condition  $s_{c,(i-1)}^{t+1}$  during the swing phase of step  $(i - 1)$ .

$$Mc(\mathbf{s}_{c,(i-1)}) = Max\{s_{c,(i-1)}^{t+1} | s_{c,(i-1)}^{t+1} \in \mathbf{s}_{c,(i-1)}\} \quad (7)$$

In Fig. 2, the  $Mc$  point is inside the blue circle with  $Mc$  label.

We define  $Md(\mathbf{s}_{d,(i-1)})$  as a maximum value of delay of the stance condition  $s_{d,(i-1)}^{t+1}$  during the swing phase of step  $(i - 1)$ .

$$Md(\mathbf{s}_{d,(i-1)}) = Max\{s_{d,(i-1)}^{t+1} | s_{d,(i-1)}^{t+1} \in \mathbf{s}_{d,(i-1)}\} \quad (8)$$

In Fig. 2, the  $Md$  point is inside the yellow circle with  $Md$  label.

The dynamic threshold  $th^i$  of step  $i$  is obtained:

$$th^i = Mc(\mathbf{s}_{c,(i-1)}) - Md(\mathbf{s}_{d,(i-1)}) \quad (9)$$

where, the initial value of  $th^0$  can be initiated by 0.8. Since  $th^i$  is a dynamic threshold, it helps the human foot motion localization algorithm adapt to speed changes of foot motion. This threshold is free from any pre-definded threshold value and

it only depends on the speed of motion. It increases when the motion speed increases and otherwise. So it can work with any people gait and any walking speed.

The dynamic human gait detection  $g_d^{t+1}$  can be obtained by:

$$g_{d.i}^{t+1} = \begin{cases} 0, & \max_{cd.i}^{t+1} \leq th^i \text{ (stance phase)} \\ 6, & \text{otherwise (swing phase)} \end{cases} \quad (10)$$

when  $g_{d.i}^{t+1} = 0$  it is in the stance phase, and  $g_{d.i}^{t+1} = 6$  it is in the swing phase.

---

**Algorithm 1: DYNAMIC GAIT PHASE (DGP) DETECTION**

---

**Input:** Real-time acceleration, angular rate vectors at discrete times  $t + 1$  of step  $i$  in IMU body system  $(a_{b.i}^{t+1}, w_{b.i}^{t+1})$

**Output:** *True:Stance Phase, False:Swing Phase*

```

1 if  $t + 1 \geq 2s + 1$  then
2    $j \leftarrow t$ 
3   while  $(j \leq t) \text{ and } (j \geq (t - s))$  do
4      $k \leftarrow (j - s)$ 
5     while  $k \leq j$  do
6        $a_{ave.i}^j \leftarrow a_{ave.i}^j + a_{b.i}^k$ 
7        $k \leftarrow (k + 1)$ 
8      $a_{ave.i}^j \leftarrow \frac{1}{2s + 1} a_{ave.i}^j$ 
9      $(a_{local.i}^{t+1})^2 \leftarrow (a_{local.i}^{t+1})^2 + (a_{b.i}^{t+1} - a_{ave.i}^j)^2$ 
10     $j \leftarrow (j - 1)$ 
11     $(a_{local.i}^{t+1})^2 \leftarrow \frac{1}{2s + 1} (a_{local.i}^{t+1})^2$ 
12 else
13    $j \leftarrow t$ 
14    $k \leftarrow 0$ 
15   while  $k \leq j$  do
16      $a_{ave.i}^j \leftarrow a_{ave.i}^j + a_{b.i}^k$ 
17      $k \leftarrow (k + 1)$ 
18    $(a_{local.i}^{t+1})^2 \leftarrow \frac{1}{k + 1} a_{ave.i}^j$ 
19  $d_{g.i}^{t+1} \leftarrow |a_{local.i}^{t+1} - a_{local.i}^t| + |a_{m.i}^{t+1} - a_{m.i}^t| + |w_{m.i}^{t+1} - w_{m.i}^t|$ 
20  $s_{c.i}^{t+1} \leftarrow \frac{d_{g.i}^{t+1} + d_{g.i}^t + d_{g.i}^{t-1} + d_{g.i}^{t-2} + d_{g.i}^{t-3}}{5}$ 
21  $s_{d.i}^{t+1} \leftarrow \frac{s_{d.i}^{t-1} + s_{c.i}^{t+1}}{2}$ 
22 if  $s_{d.i}^{t+1} \leq s_{c.i}^{t+1}$  then
23    $\max_{cd.i}^{t+1} \leftarrow s_{c.i}^{t+1}$ ;
24 else
25    $\max_{cd.i}^{t+1} \leftarrow s_{d.i}^{t+1}$ ;
26  $Mc(s_{c.(i-1)}) \leftarrow \text{Max}\{s_{c.(i-1)}^{t+1} | s_{c.(i-1)}^{t+1} \in s_{c.(i-1)}\}$ 
27  $Md(s_{d.(i-1)}) \leftarrow \text{Max}\{s_{d.(i-1)}^{t+1} | s_{d.(i-1)}^{t+1} \in s_{d.(i-1)}\}$ 
28  $th^i \leftarrow (Mc(s_{c.(i-1)}) - Md(s_{d.(i-1)}))$ 
29 if  $\max_{cd.i}^{t+1} \leq th^i$  then
30   return True
31 else
32   return False

```

---

The summary of the dynamic gate phase (DGP) detection algorithm is presented in Algorithm 1. We tested this algorithm

with different walking and running speeds in the hallway on the 1st floor of the Applied Research Facility (ARF) building, University of Nevada, Reno (UNR) campus. The detection result of swing and stance phases detection by this DGP detection algorithm is shown in Fig. 3. In this figure, the result for

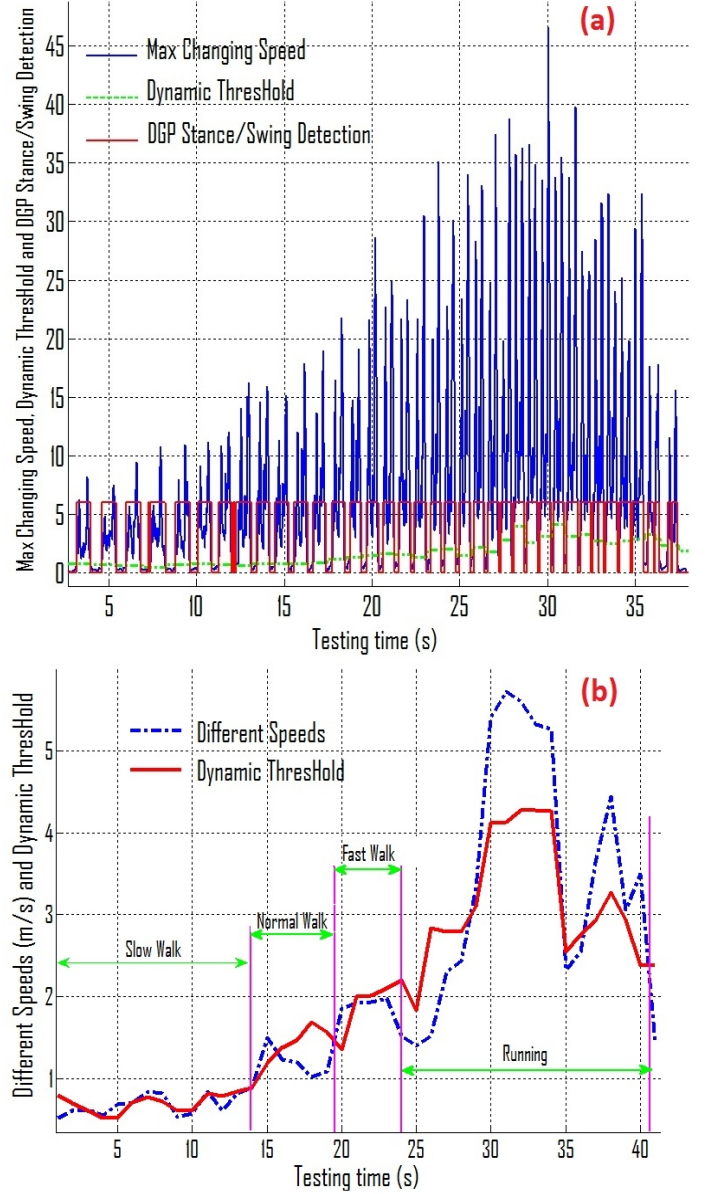


Fig. 3. Dynamic Gait Phase Detection with different speeds

different speeds: fast walk (1.92 m/s), normal walk (1.38 m/s), slow walk (0.85 m/s) and slow run (5.7 m/s) are shown for the nearly 40s moving duration. The peaks of Max Changing Speed (blue line in Fig. 3 (a)) are clearly different by different speeds. The values of dynamic threshold (green line in Fig. 3(a)) are changed definitely after each gait circle of different speeds. And the human gait phase detection (red line in Fig. 3(a)) is adaptable to different speeds. The dynamic ThresHold detected by different speeds (blue line) can be shown by the red line in Fig. 3 (b) for this testing. In this testing, we did our experiment in the hallway of the ARF building. We moved

with different speeds of walking and running. The speeds were changing as fast as explained in Fig. 3. The dynamic Threshold was detected very well and human gait phase detection was accurately detected. The accuracy of this testing is 1 error over 36 steps. It is equivalent to 2.78%.

### III. VALIDATING DGP ALGORITHM BY GROUND TRUTH SYSTEM

In this section, we validate our proposed DGP detection algorithm by using the Motion Tracking System (MTS) from Motion Analysis Corporation [13]. Because the MTS has very high accuracy, only sub-millimeter errors, we can consider this system's tracking results as a Ground Truth. The accuracy comparing between this system's result and our algorithm's result can be estimated as our algorithm's accuracy.

We setup the verified experiment relied on MTS as in Fig. 4. The configuration of this MTS included 16 passive optical cameras, in Fig. 4 (2). These cameras are mounted on the pipe system around on the wall of the Advanced Robotics and Automation (ARA) Laboratory. To warrant the MTS can track our shoe as a rigid body, we attached seven markers on it as in Fig. 4 (3).

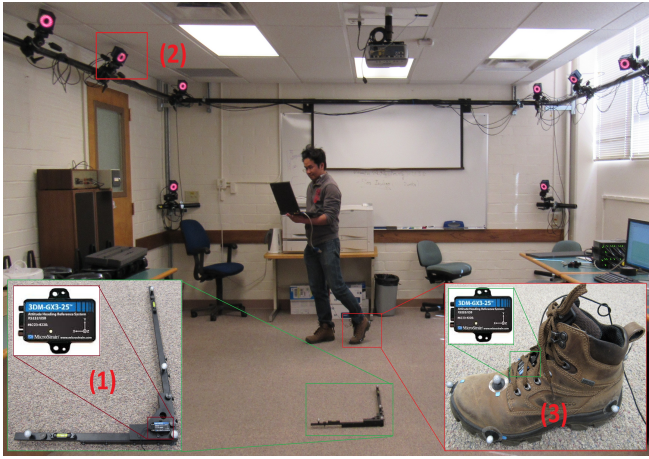


Fig. 4. Using MTS to verify for our proposed algorithm

The tracking operation of the MTS for movement of seven markers attached on the shoe as a rigid body movement shoe is demonstrated by Fig. 5.

#### A. Calibrating MTS and our proposed algorithm.

Because MTS and our proposed algorithm collect and present data in different coordinated systems, a question of validation our proposed algorithm by MTS is how to calibrate them together? The answer is that we have to transform them into NED (North East Down) system [14]–[17]. To transform MTS into NED system, we mounted a 3DM-GX3-25 IMU on a L calibration frame, a tool for calibrating and building coordinate system of the MTS. This L frame is set at the original point of the MTS coordinate system, as in Fig. 4 (1). The  $X, Y, Z$  axis of this IMU was configured equivalently to the axis of MTS system. The Euler angles *Roll* ( $\alpha$ ), *Pitch* ( $\beta$ ) and *Yaw* ( $\gamma$ ) of IMU are also the Euler angles of MTS coordinate system. The

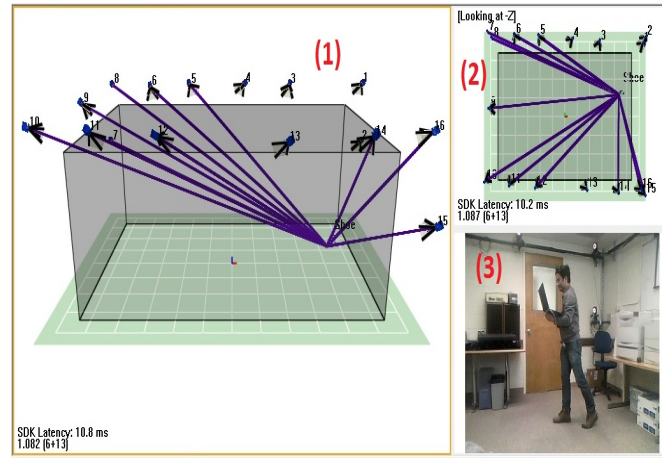


Fig. 5. MTS is tracking the shoe movement around the lab

rotation matrix,  $\mathbf{R}_M^{t+1}$ , to convert MTS data from MTS body system into MTS NED system is obtained:

$$\mathbf{R}_M^{t+1} = \begin{bmatrix} \mathbf{R}_{00} & \mathbf{R}_{01} & \mathbf{R}_{02} \\ \mathbf{R}_{10} & \mathbf{R}_{11} & \mathbf{R}_{12} \\ \mathbf{R}_{20} & \mathbf{R}_{21} & \mathbf{R}_{22} \end{bmatrix} \quad (11)$$

where,  $\mathbf{R}_{00} = c(\gamma)c(\beta)$ ,  $\mathbf{R}_{01} = c(\gamma)s(\alpha)s(\beta) - c(\alpha)s(\gamma)$ ,  $\mathbf{R}_{02} = s(\alpha)s(\gamma) + c(\alpha)c(\gamma)s(\beta)$ ,  $\mathbf{R}_{10} = c(\beta)s(\gamma)$ ,  $\mathbf{R}_{11} = c(\alpha)c(\gamma) + s(\alpha)s(\gamma)s(\beta)$ ,  $\mathbf{R}_{12} = c(\alpha)s(\gamma)s(\beta) - c(\gamma)s(\alpha)$ ,  $\mathbf{R}_{20} = -s(\beta)$ ,  $\mathbf{R}_{21} = c(\beta)s(\alpha)$ , and  $\mathbf{R}_{22} = c(\alpha)c(\beta)$ . Here,  $c$  and  $s$  are *cosine*() and *sine*() functions, respectively; and  $\alpha$ ,  $\beta$  and  $\gamma$  are obtained from IMU above [16].

We name a position collected from the MTS for a marker  $m$  at time  $t + 1$  on the shoe in MTS body frame is  $\mathbf{p}_m^{t+1} = (x_m^{t+1}, y_m^{t+1}, z_m^{t+1})$ . The transformed position  $\mathbf{p}_{mNED}^{t+1}$  of this marker in the MTS NED system is obtained:

$$\mathbf{p}_{mNED}^{t+1} = \mathbf{R}_M^{t+1} \mathbf{p}_m^{t+1}. \quad (12)$$

#### B. The experiment validates DGP algorithm by MTS.

In this section, we implement our proposed DGP detection algorithm and test it with different human motion speeds. We mount a MicroStrain 3DM-GX3-25 IMU sensor on the shoe for testing the algorithm (see Fig. 4 (3)). We implemented the algorithm by C++ language and ran them on the Hydro ROS (Robotic Operating System) platform.

The tracking space volume of the MTS in our ARA Lab is 5.2m length and 3.2m width and 3m height. We can validate DGP by MTS for separated speeds of walking: slow walk (0.86 m/s), normal walk (1.36 m/s) and fast walk (1.92 m/s).

We validate the DGP detection results by plotting both DGP's results and MTS's trajectory data on the same 2D coordinate system as presented in Fig. 6.

In Fig. 6, the blue line is MTS's  $Z$  trajectory data and red line is DGP detection results. When a foot is in Stance phase, the  $Z$  data of MTS's trajectory is the lowest position on the floor. In this phase, the DGP detection algorithm must return the Zero value for Stance phase. When foot starts to swing, the  $Z$  data of MTS's trajectory increases and DGP detection

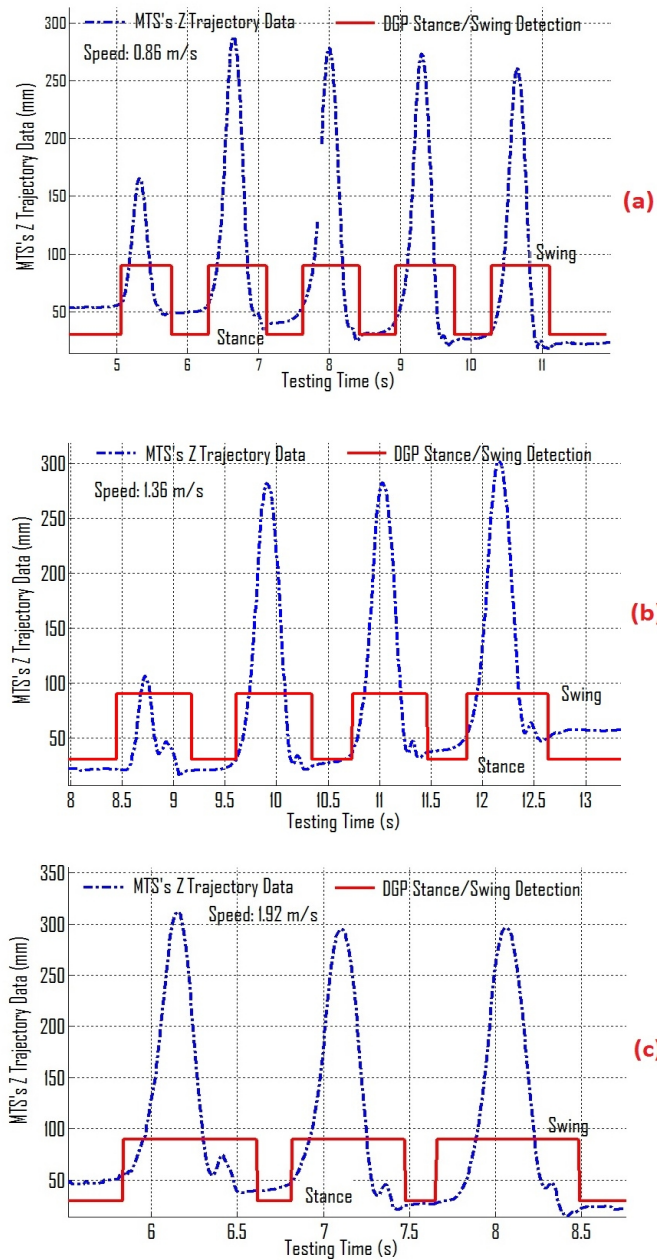


Fig. 6. Comparison of MTS's Z Trajectory and DGP detection algorithm

algorithm must detect the Swing phase. Hence, our proposed DGP detection algorithm must be matched 100% with the Z of MTS to prove that it works successfully. The results plotted in Fig. 6(a)(b)(c) have shown that they are matched together for all phases with different foot motion speeds. Hence our DGP detection algorithm has been validated correctly by MTS Ground Truth system.

#### IV. CONCLUSION

In this paper, we have proposed a Dynamic Human Gait Phase (DGP) detection algorithm for human foot motion using a single IMU device. The proposed DGP detection algorithm can accurately detect the human gait phases with different speeds of human motion like walking, random walking or

running. Moreover, our proposed algorithm can work in real-time manner to make it applicable for practical human tracking and localization applications. Experimental results have been conducted to prove the effectiveness and high accuracy of our proposed algorithm. We have applied the MTS, a Ground Truth system, to further verify our algorithm.

#### ACKNOWLEDGMENT

The authors would like to thank the University of Nevada at Reno (UNR) and National Science Foundation under grant NSF-ICorps #1535716 for their financial supports. The authors would also like to specially thank the Motion Analysis Corporation for their support of the Motion Tracking System (MTS) setup at the Advanced Robotics and Automation (ARA) Lab at UNR.

#### REFERENCES

- [1] C. Randell, C. Djallil, and H. Muller. Personal position measurement using dead reckoning. *Proc. 7th IEEE Int'l Symp. Wearable Computers, (ISWC)*, IEEE CS Press, pages 166–173, 2003.
- [2] I. Skog, P. Handel, J. Nilsson, and J. Rantakokko. Zero-velocity detection algorithm evaluation. *Biomedical Engineering, IEEE Transactions*, 57(11):2657–2666, November 2010.
- [3] A.R. Jimenez, F. Seco, J.C. Prieto, and J. Guevara. Indoor pedestrian navigation using an ins/ekf framework for yaw drift reduction and a foot-mounted imu. *IEEE Positioning Navigation and Communication (WPNC), 7th Workshop*, 2010.
- [4] X. Yun, J. Calusdian, E. R. Bachmann, and R. B. McGhee. Estimation of human foot motion during normal walking using inertial and magnetic sensor measurements. *Instrumentation and Measurement, IEEE Transactions*, 61(7):2059–2072, July 2012.
- [5] E. Foxlin. Pedestrian tracking with shoe-mounted inertial sensors. *IEEE Computer Graphics and Applications*, 1:38–46, 2005.
- [6] Q. Yuan, I. M. Chen, and S. P. Lee. Slac: 3d localization of human based on kinetic human movement capture. In *Robotics and Automation (ICRA), 2011 IEEE International Conference on*, pages 848–853, May 2011.
- [7] F. Hoffinger, R. Zhang, and L. M. Reindl. Indoor-localization system using a micro-inertial measurement unit (imu). In *European Frequency and Time Forum (EFTF)*, pages 443–447, April 2012.
- [8] H. Fourati, N. Manamanni, L. Afilal, and Y. Handrich. Position estimation approach by complementary filter-aided imu for indoor environment. In *European Control Conference (ECC)*, pages 4208–4213, July 2013.
- [9] L. Nguyen and H. M. La. Development of a smart shoe for building a real-time 3d map. *The 32nd International Symposium on Automation and Robotics in Construction and Mining (ISARC 2015)*, June 2015.
- [10] N. Corso and A. Zakhor. Indoor localization algorithms for an ambulatory human operated 3d mobile mapping system. *Remote Sensing*, 5(12):6611–6646, 2013.
- [11] Z. J. Chong, B. Qin, T. Bandyopadhyay, M. H. Ang Jr., E. Frazzoli, and D. Rus. Synthetic 2d lidar for precise vehicle localization in 3d urban environment. *IEEE International Conference on Robotics and Automation (ICRA)*, pages 1554–1559, May 2013.
- [12] H. Zhang, J. Qian, L. Shen, and Y. Zhang. Research on healthy subject gait cycle phase at different walking speeds. *Robotics and Biomimetics (ROBIO), 2012 IEEE International Conference on*, pages 1349–1354, December 2012.
- [13] Motion Analysis Corporation. Motion tracking system. <http://www.motionanalysis.com/>, 2015.
- [14] R. S. Lim, H. M. La, Z. Shan, and W. Sheng. Developing a crack inspection robot for bridge maintenance. In *Robotics and Automation (ICRA), 2011 IEEE International Conference on*, pages 6288–6293, May 2011.
- [15] W. George and II. Collins. *The Foundations of Celestial Mechanics*. The Pachart Foundation dba Pachart Publishing House and reprinted by permission, US, 2004.
- [16] R. S. Lim, H. M. La, and W. Sheng. A robotic crack inspection and mapping system for bridge deck maintenance. *Automation Science and Engineering, IEEE Transactions*, 11(2):367–378, April 2014.
- [17] H. M. La, N. Gucunski, S. K. Kee, and L. V. Nguyen. Data analysis and visualization for the bridge deck inspection and evaluation robotic system. *Visualization in Engineering*, 3(1):6, 2015.